Microstructural investigation of the recrystallization of warm-rolled tungsten

Alfonso, A.; Pantleon, W.; Luo, G.-N.; Juul Jensen, D.

Published in:
Proceedings of the Risø International Symposium on Materials Science

Publication date:
2014

Document Version
Publisher's PDF, also known as Version of record

MICROSTRUCTURAL INVESTIGATION OF THE RECRYSTALLIZATION OF WARM-ROLLED TUNGSTEN

A. Alfonso[*,#], W. Pantleon[*,**,#], G.-N. Luo[***,#], D. Juul Jensen[****,#]

[*] Section of Materials and Surface Engineering, Department of Mechanical Engineering, Technical University of Denmark, 2800 Lyngby, Denmark
[**] Association EURATOM – DTU
[***] Fusion Reactor Materials Science and Technology Division, Institute of Plasma Physics, Chinese Academy of Sciences, 230031 Hefei, Anhui, China
[****] Danish-Chinese Center for Nanometals, Section for Materials Science and Advanced Characterization, Department of Wind Energy, Technical University of Denmark, Risø Campus, 4000 Roskilde, Denmark
[#] Sino-Danish Center for Education and Research

ABSTRACT

Annealing of a 90% warm-rolled tungsten plate with an average spacing between deformation-induced dislocation boundaries in the nanometer/submicron range is investigated. Focus is on the changes in microstructure and texture during annealing at 1200 °C. Electron backscatter diffraction (EBSD) is used for experimental characterization of a series of samples isothermally annealed for different times up to 25 h. The evolving texture is compared to theoretical predictions; it is found that the recrystallization texture of the present material is largely determined by nucleation.

1. INTRODUCTION

Pure tungsten is considered a potential candidate material for the plasma-facing first wall and the divertor of fusion reactors. An important reason for this choice is the high melting point (3422 °C) of tungsten, which makes tungsten excellent to withstand the high heat loads and temperature gradients which are intrinsic features of fusion reactors (Wirtz, Linke, Pintsuk, Rapp and Wright 2012). Furthermore, the microstructure and texture of the material are important design parameters. For example, refinement of the grain size may lead to improved radiation resistance (Kurishita, Matsuo, Arakawa, Okano, Watanabe, Yoshida, Sakamoto, Kobayashi, Nakai, Hatakeyama,

Shikama, Ueda, Takida, Kato, Ikegaya, Torikai and Hatano 2014). It has been observed also that the crystallographic orientations of the grains are critical in determining the amount and structure of blistering on the surface when exposed to a high flux plasma (Xu, Zhang, Yuan, Fu, Godfrey, De Temmerman, Liu and Huang 2013).

The aim of the present work is to study the microstructure and texture development of a warm-rolled tungsten plate during isothermal annealing at high temperatures. The plate chosen for this work was warm-rolled to 90% thickness reduction, which is industrially feasible and leads to a refined deformation microstructure with an average boundary spacing in the nanometer (submicrometer) range. Both, deformation microstructure and texture are described, and nucleation and growth of grains during recrystallization are studied. The recrystallization temperature may or may not affect the microstructural development, as has been observed in aluminum at different strains (Vandermeer and Juul Jensen 1998; Vandermeer, Wu and Juul Jensen 2009). Whether this is the case for the present pure tungsten material is the topic of a planned publication. The present study will focus on recrystallization at 1200 °C, which is the maximum temperature expected for the first wall during accidental conditions (e.g. loss of coolant), with the normal operation temperature being 600 °C (Hermsmeyer, Norajitra, Di Pace, Giancarli, Forrest, Taylor, Cook, Ward, Sardain and Maisonnier 2005).

2. EXPERIMENTAL

A warm-rolled plate of 99.95% pure tungsten was received from Advanced Technology & Materials Co., Ltd., Beijing. The plate had been manufactured from tungsten powder by cold-isostatic pressing and sintering under a hydrogen atmosphere at 2300 °C for 6 h. In a final step, the plate had been warm-rolled at a temperature of approximately 1000 °C in several passes to a thickness reduction of 90%. Small specimens of about $3\times4\times8$ mm^3 were cut from the plate. Only specimens far from the edges of the rolled plate were investigated further.

These specimens were isothermally annealed in a universal high temperature tube furnace Nabertherm RHTC 80-230/15 for different times at 1200 °C. Protection of the specimen against oxidation was required to avoid formation of volatile WO_3. The individual specimens were encapsulated in glass ampoules. The ampoules, each containing a single specimen, were floated with argon, evacuated and finally sealed. The specimens were put in the pre-heated furnace, removed after the desired annealing time and cooled to room temperature by air-cooling. Specimens which showed any indication of oxidation after the heat treatment were discarded.

For further investigations, a fresh surface perpendicular to the rolling plane comprising the rolling direction (RD) and the normal direction (ND) was prepared. The microstructure on these sections was characterized by determining local orientations using electron backscatter diffraction (EBSD). Specimens for such microstructural characterization were first mechanically polished and then chemically polished with an Oxide Particle Suspension (OPS). Finally, the samples were electropolished with NaOH 3% wt. for 45 s at a constant voltage of 10 V.

For electron backscatter diffraction, a FEI Helios Nanolab™ 600 with an EDAX Hikari Camera as detector was used. The OIM 5TM software from EDAX TSL was used to index the recorded electron backscatter patterns. The orientation data gathered on square grids of different step sizes were finally analyzed using HKL Channel 5 software. The presented orientation maps are colored

according to the crystallographic direction aligned with ND. Orientation distribution functions (ODFs) are calculated from the individual orientations using a Gaussian spread function with 5º half width by series expansion in generalized spherical harmonics truncated at order 22.

Recrystallized regions in the partially recrystallized samples were determined from the orientation data using the in-house software DRG (Wu and Juul Jensen 2008) based on three criteria: i) the internal misorientation within a recrystallized nucleus/grain is less than 1°, ii) the area of a nucleus/grain is larger than 8 pixels corresponding to 72 μm^2 or 200 μm^2 (for maps with 3 μm or 5 μm step size respectively) and iii) the nucleus/grain is at least partially surrounded by high angle boundaries with misorientations larger than 15°. The volume fraction *X* of recrystallized material is determined as the area fraction of all recrystallized nuclei/grains detected in the orientation map.

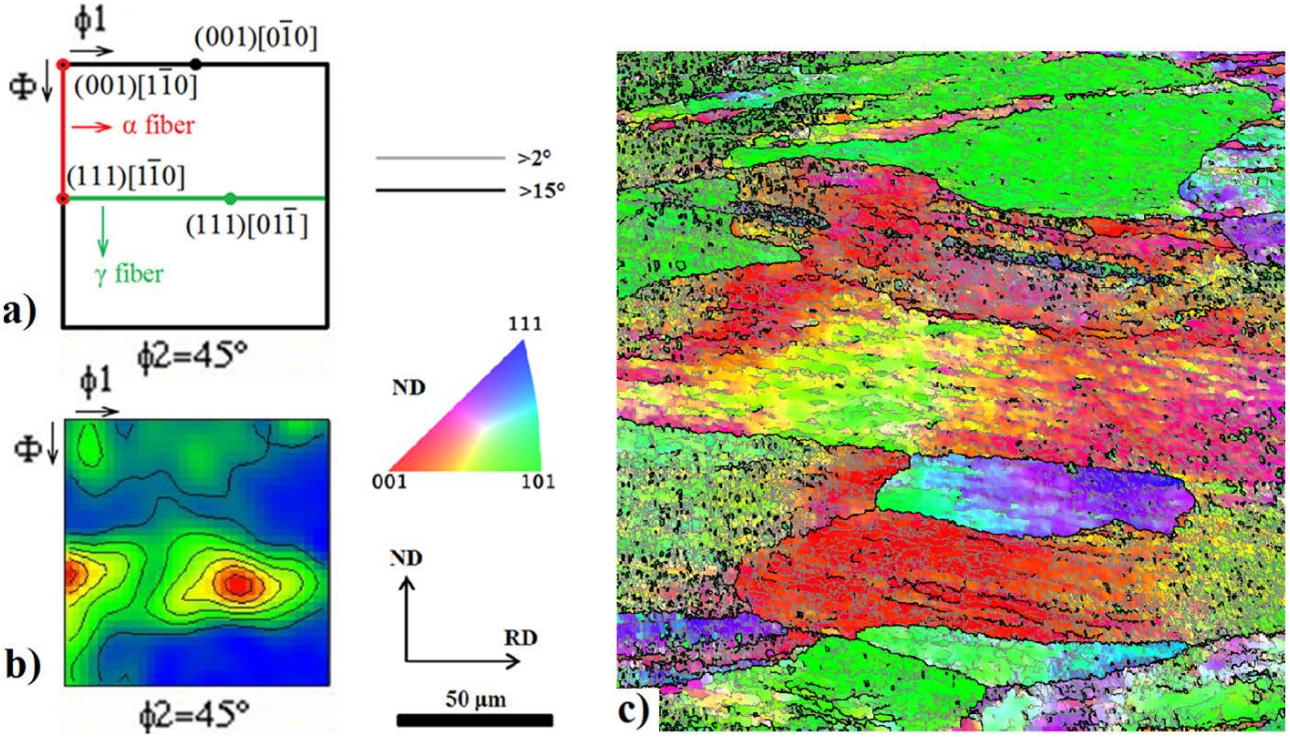

Fig. 1. Tungsten warm-rolled to 90% thickness reduction: a) Sketch of the $\phi_2 = 45°$ section of orientation space indicating the main components of a typical bcc rolling texture: the α fiber (red) and the γ fiber (green), as well as some of their components $(001)[1\bar{1}0]$, $(111)[1\bar{1}0]$, $(111)[01\bar{1}]$ together with a typical recrystallization component $(001)[0\bar{1}0]$. b) ϕ_2=45º section of the orientation distribution function (ODF) calculated from the orientation data from an EBSD map sized 1404×1404 μm^2 obtained with a 3 μm step size (the corresponding orientation map is not shown); contour lines indicate the orientation density in multiples of a random distribution from 1 to 6. The maximum orientation density (red) is 6.4. c) Orientation map obtained by EBSD with a 0.2 μm step size, where grey lines represent low angle boundaries (LABs) and black lines high angle boundaries (HABs). Inverse pole figure (IPF) coloring of the normal direction is used.

3. RESULTS AND DISCUSSION

3.1 Deformation structure. The results on the as-received warm-rolled condition are summarized in Fig. 1. Information about the texture is gained from a large orientation map of 1404×1404 μm^2 gathered with a large step size of 3 μm. In the warm-rolled state, the texture of the present material is a typical bcc rolling texture, with pronounced orientation densities along the so-called γ and α fibers ({111}<uvw> and {hkl}<110>, respectively, cf. Fig. 1a) although the balance between the orientation densities is shifted towards a dominating γ fiber with only a weak α fiber (see Fig. 1b). In fact, it is essentially only the {111}<110> component which is observed as a clear peak along the α fiber, and this component is evenly shared with the γ fiber. The second clear peak seen along the γ fiber corresponds also to {111}<110>. The observed maximum orientation densities are not very high, which is typical for high temperature rolling of pure and low-alloyed bcc transition metals (Raabe and Lücke 1994). In contrast, cold-rolling of W has been shown to lead to stronger textures in which the {001}<110> component dominates (Pugh 1958; Park, Lee and Gottstein 1998; Raabe and Lücke 1994). For the present sample, only a rather weak peak with an orientation density below 2 times random is seen for this orientation (see Fig. 1a and b).

The warm-rolled microstructure is illustrated by an orientation map of a smaller area obtained with a fine step size of 0.2 μm shown in Fig. 1c. It consists of large grains elongated along the rolling direction (RD) with an aspect ratio of approximately 3.4. As Fig. 1c reveals, these grains are subdivided by deformation-induced low and high angle boundaries caused by the warm-rolling. The subdivision seems to depend on the orientation of the grains; some grains appear less subdivided than other grains. The average spacing between boundaries with misorientation angles larger than 2° is 720 nm and 820 nm along RD and ND, respectively.

3.2 Recrystallization structure. After annealing for 25 h at 1200 °C, the sample is fully recrystallized; the results obtained by EBSD for this recrystallized state are summarized in Fig. 2. The microstructure consists of grains slightly elongated along RD with an aspect ratio of 1.2 (Fig. 2a). The grain size distribution is broad as seen from the observed grain area distribution in Fig. 2b with a maximum apparent grain area of 108,000 μm^2 and an average apparent grain area of 12,000 μm^2. Such wide grain size distributions are typical for hot-deformed samples. The texture (cf. Fig. 2c) consists of some remaining preferred orientations along the γ fiber and a near cube component (near {100} <001>, see Fig. 1a). It has to be noted that the area from which the recrystallization texture is determined is only 1500×1500 μm^2 (Fig. 2a). Work is under way to measure the texture from a much larger area.

Theories are available which successfully predict how the typical {001}<110> component seen in cold-rolled W transforms during recrystallization into a weak near cube texture (Lee 1995; Park, Lee and Gottstein 1998). According to these models, the weakening of the texture is related to the elastic isotropy of tungsten, which allows the {001}<110> components to transform into various recrystallization texture components by <110> rotations. In particular, the near-cube components are argued to be caused by selective and rapid consumption of the {001}<110> rolling component (Park, Lee and Gottstein 1998). As described above, the deformation texture of the present material is different from the simple {001}<110> texture assumed in the model. It is thus relevant to quantify orientation effects for both nucleation and growth of recrystallizing grains in partially recrystallized samples.

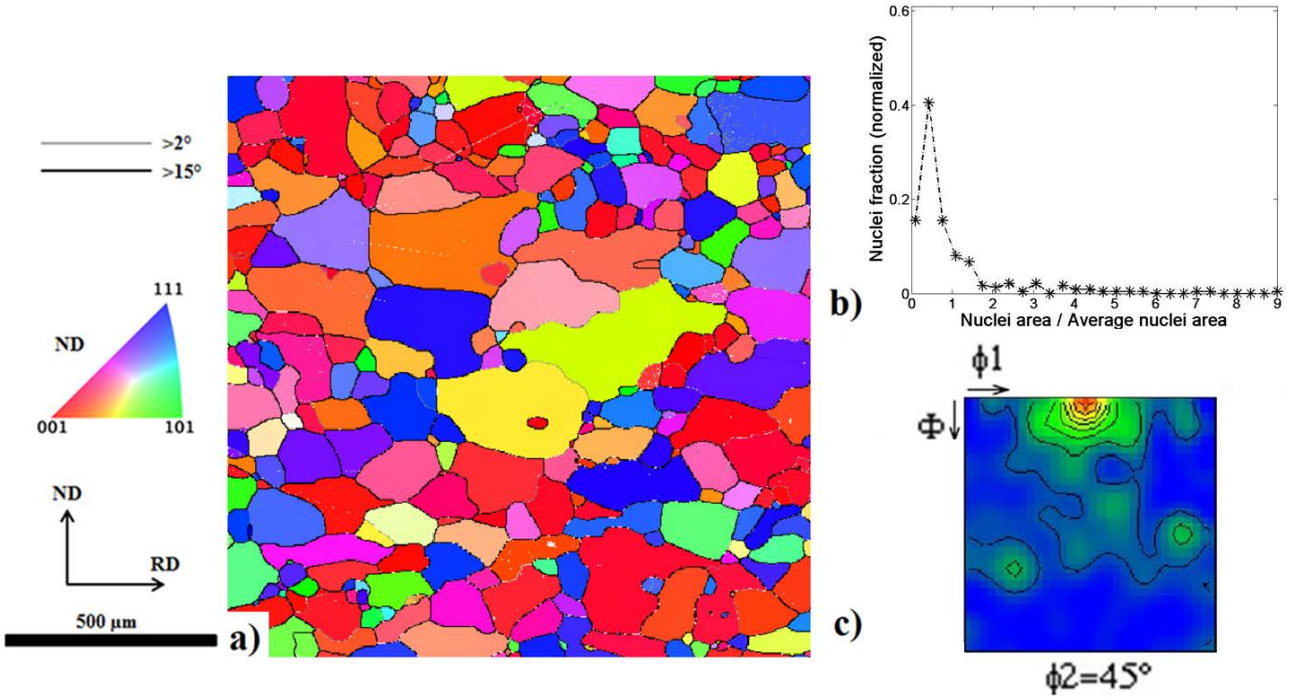

Fig. 2. Fully recrystallized tungsten (warm-rolled to 90% thickness reduction and annealed for 25 h at 1200 °C): a) Orientation map obtained by EBSD with a 3 µm step size covering an area 1500×1500 µm^2. IPF coloring of the normal direction is used. b) Normalized apparent grain area distribution showing grains up to 9 times larger than the average grain size. c) ϕ_2=45º section of the ODF calculated from the orientation data in a); contour lines indicate the orientation density in multiples of a random distribution from 1 to 8. The maximum orientation (red) is 8.8. A broad cube component {100} <001> can be observed.

3.3 Partially recrystallized structure. The orientation map for a sample annealed for 7 h at 1200 ºC shown in Fig. 3a illustrates an early stage of recrystallization: nuclei develop relatively well spatially-distributed in the deformed matrix. Some weak clustering along RD is observed which is not surprising, taking into account the orientation dependence of the deformation-induced subdivision of the deformed grains discussed in section 3.1.

The orientation distribution of the nuclei is quite spread with a slight preference for near-cube orientations. This is illustrated in Fig. 3b, in which the orientations of in total 184 nuclei observed in the three samples annealed for the shortest times showing recrystallization (i.e. 7 h, 8 h, and 8.5 h corresponding to recrystallized volume fractions of 5%, 8%, and 9%, respectively) are presented in a {111} pole figure. Although it may not be statistically representative, when converted into an ODF (see Fig. 3c), it appears that the orientation distribution of the nuclei/grains at these early recrystallization stages closely resembles that of the fully-recrystallized texture (compare Fig. 2c) and shows again the slight preference of the near cube orientation {100} <001>.

3.4 Growth. During recrystallization the recrystallized grains grow into the deformed matrix by migration of the boundaries surrounding the nuclei, while no migration is expected where nuclei boundaries impinge upon each other. Average growth rates are often estimated by measuring the average size of the nuclei/recrystallized grains for samples annealed at different times. The results hereof are presented in Fig. 4a, which show that the average size (measured by the mean chord length) increases linearly with annealing time up to 15 h, corresponding to a recrystallized fraction

of 52%. After that, the increase in chord length with time decreases, as expected from severe impingement between the recrystallizing grains. The increase in average intercept length during the early stages of recrystallization is approximately 5 μm/h, being very similar along RD and ND. The size advantage of 20 μm of the chord length along RD compared to the one along ND (corresponding to an aspect ratio of 1.2 in the fully-recrystallized state) is actually observed soon after nucleation and maintained during the entire recrystallization process. Assuming, that (almost) spherical grains grow freely without impingement restrictions and no new nuclei appear, the average intercept length increase rate can be converted to a boundary migration rate/growth rate by dividing with a stereological factor 4/3 (Vandermeer and Juul Jensen 1998). In this manner, the present data suggest a growth rate of about 3.8 μm/h for the early stage of recrystallization.

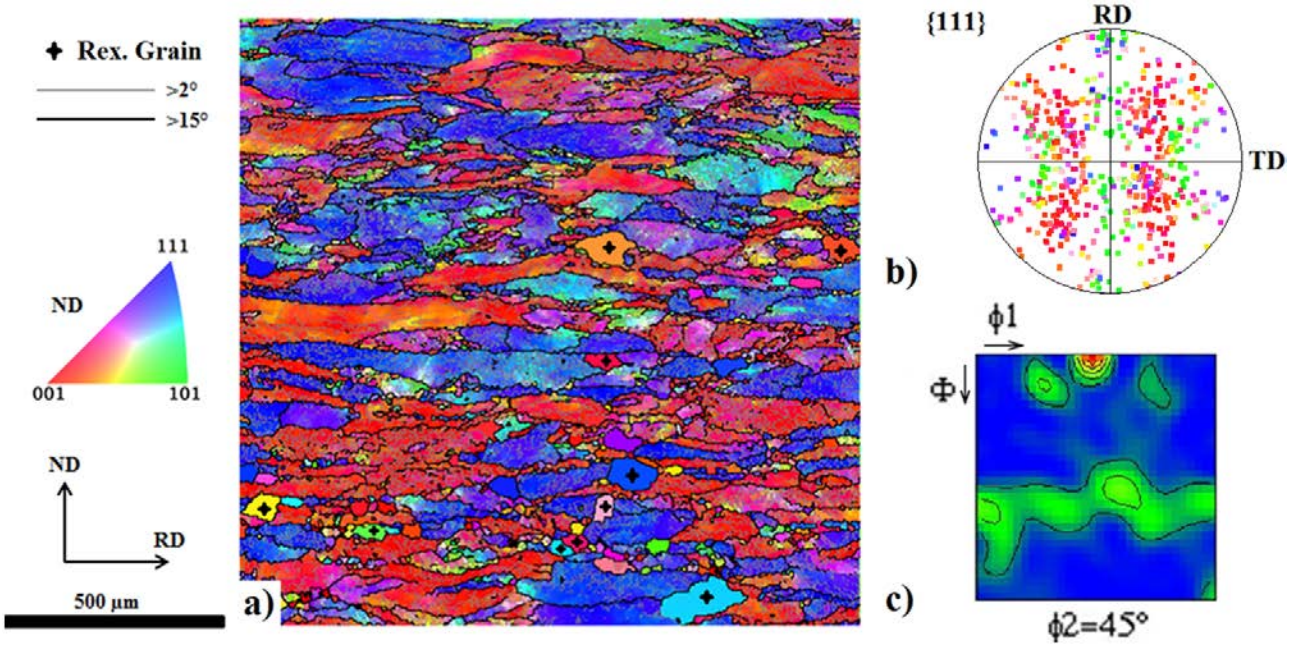

Fig. 3. Partially recrystallized tungsten (warm-rolled to 90% thickness reduction and annealed for 7 h at 1200 °C): a) Orientation map obtained by EBSD with a 3 μm step size covering an area 1368×1368 μm^2. IPF coloring of the normal direction is used. Ten of the recrystallizing grains are marked by cross symbols. b) {111} pole figure presenting the individual orientations of the 184 nuclei present in the maps corresponding to the three shortest annealing times (7 h, 8 h, 8.5 h), with IPF coloring along ND. c) ϕ_2=45º section of the ODF calculated from the orientations of the 184 nuclei; contour lines indicate the orientation density in multiples of a random distribution from 1 to 5. The maximum orientation (red) is 5.8.

A much more precise (but also more labor-intense) method to determine growth rates during recrystallization has been proposed by Cahn and Hagel (1993). The Cahn Hagel method takes the impingement between recrystallized grains properly into account by considering the density S_V of boundary surfaces between nuclei and the deformed matrix. For the present samples, the average growth rate $\left(dX/dt\right)/S_V$ is accordingly found to be approximately 4.5 μm/h. This value is slightly larger than that determined from the simple linear intercept method. This is expected because, as is obvious in Fig. 3a, some nuclei already impinge upon each other at the earliest stage of recrystallization, so not all boundaries are free to migrate.

As discussed in section 3.2, the model describing the texture transformation and the development of a weak cube component incorporates a selective and rapid consumption of the {001}<110> rolling component during growth. This is analyzed here by calculation and inspection of the ODF for only the deformed part of the microstructure in the partially recrystallized state. An example is shown in Fig. 4b, where the $\phi_2 = 45°$ section of the ODF for the sample annealed for 13 h corresponding to a recrystallized fraction of 41% is presented. The figure reveals that the texture of the deformed matrix in this partially recrystallized state consists mostly of {111}<011> and {001}<110> components. The intensities of these two components are largely unaltered by the 41% recrystallization, whereas the other components of the deformation texture (e.g. along the γ fiber) have been consumed by recrystallizing grains. For the present sample with its somewhat unusual deformation texture, it is therefore apparent that preferential consumption of {001}<110> is not the dominating mechanism.

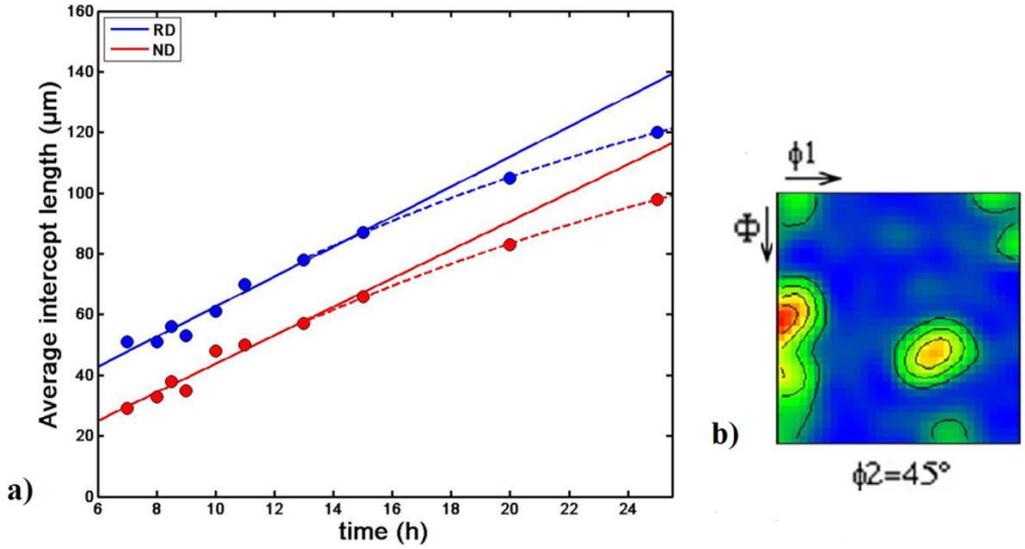

Fig. 4. a) Average size of the nuclei/recrystallizing grains measured as average intercept lengths along RD (blue) and ND (red). The average size fits a linear relationship, except for the two longest annealing times of 20 h and 25 h, where grain impingement limits the growth of the nuclei substantially. b) ϕ_2=45º section of the ODF calculated from the non-recrystallized (still deformed) part of the microstructure of a partially recrystallized ($X = 0.41$) sample annealed for 13 h at 1200 °C; contour lines indicate the orientation density in multiples of a random distribution from 1 to 4. The maximum orientation (red) is 4.9. Mainly {111}<011> and {001}<110> components are seen.

4. CONCLUSIONS

For the investigated tungsten plate warm-rolled to 90% thickness reduction, annealing at 1200 °C leads to recrystallization whereby the microstructure is significantly coarsened. In the deformed state the distance between deformation-induced dislocation boundaries (including all boundaries with misorientations above 2°) is 720 nm and 820 nm along RD and ND, respectively, whereas in the recrystallized state the chord length of the recrystallized grains are 120 μm and 100 μm along the same directions. The texture changes from a weak bcc rolling texture with dominating γ fiber

components to a near-cube texture {100}<001>. This textural change is to a large extent determined by the nucleation process whereby nuclei with orientations very similar to the recrystallization texture form. During growth, there is a weak preference for migration through deformed grains with orientations other than {111}<011> and {001}<110>. This evolution is different from that predicted previously for cold-rolled W where preferential growth into {001}<110> is assumed.

ACKNOWLEDGEMENTS

The authors gratefully acknowledge the Sino-Danish Center for Education and Research and the European Fusion Development Agreement for financial support and Advanced Technology & Materials Co., Ltd., Beijing, for providing the material. We also acknowledge Lars Lorentzen from the Department of Wind Energy, Technical University of Denmark, for preparation and encapsulation of the samples.

REFERENCES

Cahn, J.W., and Hagel, W.C. (1963). Divergent pearlite in a manganese eutectoid steel. Acta Metall. 11, 561-574.

Hermsmeyer, S., Norajitra, P., Di Pace, L., Giancarli, L., Forrest, R., Taylor, N.P., Cook, I., Ward, D.J., Sardain, P., and Maisonnier, D. (2005). European fusion power plant studies. Fusion Sci. Technol. 47, 384-392.

Kurishita, H., Matsuo, S., Arakawa, H., Okano, H., Watanabe, H., Yoshida, N., Sakamoto, T., Kobayashi, S., Nakai, K., Hatakeyama, M., Shikama, T., Ueda, Y., Takida, T., Kato, M., Ikegaya, A., Torikai, Y., and Hatano, Y. (2014). Current status of nanostructured tungsten-based materials development. Phys. Scr. T159, 1-7.

Lee, D.N. (1995). The evolution of recrystallization textures from deformed textures. Scr. Metall. Mater. 32, 1689-1694.

Park, Y.B., Lee, D.N., and Gottstein, G. (1998). The evolution of recrystallization textures in body centered cubic metals. Acta Mater. 46, 3371-3379.

Pugh, J.W. (1958).Temperature dependence of preferred orientation in rolled tungsten. Trans. A.I.M.E. 212, 637-642.

Raabe, D., and Lücke, K. (1994). Rolling and annealing textures of bcc metals. Mater. Sci. Forum 280, 597-610.

Vandermeer, R.A., and Juul Jensen, D. (1998). The migration of high angle grain boundaries during recrystallization. Interf. Sci. 6, 95-104.

Vandermeer, R.A., Wu, G.L., and Juul Jensen, D. (2009). Microstructural path model and strain dependence of recrystallization in commercial aluminium. Mater. Sci. Technol. 25, 403-406.

Wirtz, M., Linke, J., Pintsuk, G., Rapp, J., and Wright, G.M. (2012). Influence of high flux hydrogen-plasma exposure on the thermal shock induced crack formation in tungsten. J. Nucl. Mater. 420, 218-221.

Wu, G.L., and Juul Jensen, D. (2008). Automatic determination of recrystallization parameters based on EBSD mapping. Mater. Charact. 59, 794-800.

Xu, H.Y., Zhang, Y.B., Yuan, Y., Fu, B.Q., Godfrey, A., De Temmerman, G., Liu, W., and Huang, X. (2013). Observations of orientation dependence of surface morphology in tungsten implanted by low energy and high flux D plasma. J. Nucl. Mater. 443, 452-457.